Clim Dyn
DOI 10.1007/s00382-007-0363-5

# Response of the tropical Pacific to changes in extratropical clouds

**Marcelo Barreiro · S. George Philander**

Received: 24 April 2007 / Accepted: 26 December 2007


**Abstract** A decrease in cloud cover over higher latitudes—a decrease in the extratropical albedo—especially over the Southern Ocean, can result in an extratropical and tropical warming with the intensity of the equatorial cold tongues in the Pacific and Atlantic basins decreasing. These results, obtained by means of a coupled ocean–atmosphere model of intermediate complexity that allow the prescription of atmospheric cloud cover, are relevant to future global warming, and also to conditions during the Pliocene some 3 million years ago. The mechanisms responsible for the response of the tropics to changes in the extra-tropics include atmospheric and oceanic connections. This tropical adjustment can be interpreted from the constraint of a balanced heat budget for the ocean: A change in the albedo of the Southern Hemisphere causes the ocean to lose less heat there, so that it has to gain less heat in the tropics. As a consequence the cold tongues are reduced, particularly in the eastern Pacific where a decrease in the zonal tilt of the equatorial thermocline significantly weakens the east-west sea surface temperature gradient. The total adjustment time scale of the equatorial Pacific to the extratropical perturbation is of the order of interdecadal to centennial time scales, and thus represents a new mechanism of rapid climate change.

M. Barreiro (✉)
Igua 4225, Instituto de Física, Facultad de Ciencias,
Universidad de la República, 11400 Montevideo, Uruguay
e-mail: barreiro@fisica.edu.uy

S. G. Philander
Atmospheric and Oceanic Sciences, Department of Geosciences,
Princeton University, Princeton, NJ, USA

S. G. Philander
Department of Oceanography, University of Cape Town,
Rondebosch, 7701 Cape Town, South Africa

**Keywords** Tropical Pacific · Heat budget · Cloud albedo · Tropical–extratropical connections · Rapid climate changes

## 1 Introduction

The influence of changes in extratropical conditions on the tropics is of great interest in connection with future global warming. How will a warming of high latitudes, that causes the melting glaciers, and changes in rainfall patterns, affect tropical conditions? Studies that address this question focus mainly on two issues: the consequences of a freshening of the surface waters of the northern Atlantic Ocean; and the effects of a warming of the surface waters of the ocean in higher latitudes. This paper deals with a third factor, the impact of changes in the clouds, and hence the albedo, in high latitudes.

The addition of large amounts of freshwater onto the surface waters of the far northern Atlantic, corresponding to a sudden and catastrophic melting of icebergs for example, can have a significant influence on the tropics, by means of both an atmospheric bridge and an oceanic tunnel. Initial studies focused on the deep component of the tunnel, the thermohaline circulation (e.g. Manabe and Stouffer 1995; Rahmstorf 1995; Vellinga and Woods 2002; Stouffer et al. 2006; Barreiro et al. 2007). Recent explorations of the shallow component, associated with the wind-driven circulation of the ventilated thermocline, include those of Gu and Philander (1997), Boccaletti et al. (2004) and Sun et al. (2004). Of central importance in the latter studies is the constraint of a balanced heat budget for the ocean. The heat that the oceans gain, especially in regions of equatorial upwelling in the Atlantic and Pacific, is balanced by the loss in the extratropics. Boccaletti et al. (2004) showed that, even under constant wind stress forcing, a decrease in the loss of heat in high latitudes can decrease the gain at the equator by inducing a deepening of the equatorial thermocline, and hence a rise in equatorial sea surface temperatures. Interactions between the ocean and atmosphere (of the type that characterizes El Niño) can then amplify the signal. See Barreiro et al. (2007) for a review.

What will be the impact of a warming of the surface waters of the ocean in high latitudes? Liu and Yang (2003), Zhang et al. (2005), and Yang and Liu (2005) address this question. In their model, Yang and Liu (2005, hereafter YL05) increase sea surface temperatures by 2 K poleward of 30° latitude in both hemispheres and find that the tropical ocean warms up to 1 K. They explain this result in terms of an atmospheric bridge that accounts for 67% of the equatorial warming (including tropical ocean–atmosphere interactions) and an oceanic tunnel that explains the remainder. They further show that the tropics are influenced mainly by the prescribed sea surface temperatures in the southern hemisphere, apparently because that hemisphere has the larger ocean surface area. The tropical response is not a uniform warming because it includes a slight increase in the gradient of sea surface temperature along the equator, apparently a consequence of the "ocean dynamical thermostat" (Clement et al. 1996).

A feature common to the various coupled ocean–atmosphere models mentioned above—independent of whether the surface waters are freshened or warmed—is the relative smallness of the changes in radiation fluxes at the top of the atmosphere (TOA). The reasons for the very modest changes in the Earth's albedo in these experiments are unclear. This is troubling because albedo depends on clouds, which are the largest source of uncertainty in climate models. Can we assume that the cloud albedo will remain essentially unchanged in future warmer climates?

The available evidence suggests that, during warm paleo-climates, the extratropical clouds had a distribution and had optical depth properties different from those of the clouds of today (Walker 1995; Sloan and Pollard 1998; Kirk-Davidoff et al. 2002). Today there are indications that biological activity over the Southern Ocean can regulate the properties of stratiform clouds, and can strongly affect the short-wave radiative flux at the top of the atmosphere (Meskhidze and Nenes 2006). These results motivate the present study, which addresses the climate impact of changes in the extratropical clouds, particularly on the mean state of the tropical Pacific Ocean.

The atmospheric adjustment to changes in cloud cover can alter the oceanic circulation by modifying the wind stress and surface heat fluxes. The ocean in turn affects the atmosphere, bringing ocean–atmosphere interactions into play. In this paper we show that the net result of reduced extratropical albedo can be a reduction in the poleward transport of heat, in both the ocean and atmosphere. As in the case of the model of Yang and Liu (2005), the southern hemisphere exerts the dominant influence on the equatorial response. However, the sea surface temperature gradient along the equator is reduced in this study of the effects of decreased extratropical albedo, a result consistent with the argument that a decrease in heat loss in high latitudes has to be accompanied by a decrease in the heat gained at the equator.

How do we test the validity of these results? If different models give different results, how do we determine which are correct? Certain aspects of paleo-climates provide invaluable tests for the models. Of special interest is the Pliocene, some 3 million years ago, when extratropical regions were about 3–6 K warmer than today, and when cold surface waters were absent from the equatorial Pacific and coastal upwelling regions. Can the previous results mentioned here, and the new results presented here, explain the conditions during the Pliocene? We return to this question in the final discussion section.

The paper is organized as follows. The next section describes the model that is used in this study. Section 3 analyzes the results when the global extratropical cloud cover (albedo) is reduced. Sections 4 and 5 concern the response of the tropics to localized cloud cover reductions in the North Pacific and Southern Ocean, respectively. Sections 6 and 7 address the role of the atmosphere and the ocean, respectively. For a summary of the results see the final Sect. 8.

## 2 Model and experiments

We use the coupled atmosphere–ocean–sea ice model known as ECBILT-CLIO (version 3). The atmospheric component (ECBILT) is quasi-geostrophic, is global, has three vertical levels, and has a horizontal resolution corresponding to T21 (Opsteegh et al. 1998). The equation for the tendency of the quasi-geostrophic potential vorticity includes terms that represent the ageostrophic contributions in the vorticity equation and the advection of temperature by the ageostrophic wind. The inclusion of these terms are necessary to simulate the Hadley circulation quantitatively correctly. This has large consequences for the strength and position of the jet stream and for the extratropical transient eddy activity (Opsteegh et al. 1998). The hydrological cycle is closed over land by a land bucket model. The ocean–sea ice component (CLIO) is an ocean general circulation model with a free surface, plus a thermodynamic/dynamic sea-ice model (Goose and Fichefet 1999). CLIO has a horizontal resolution of $3° \times 3°$ and 20 vertical levels (13 levels in the upper 1,000 m). The coupled model is run without heat flux correction, but includes a weak freshwater correction that reduces the precipitation over the

Atlantic and Arctic basins and redistributes this amount uniformly over the Pacific Ocean in order to get a realistic salinity distribution.

The ECBILT-CLIO has been used extensively to study paleo-climates and the large-scale ocean circulation (e.g., Knutti et al. 2004; Timmermann and Goosse 2004a; Timmermann et al. 2004b). Moreover, it has been found that the simulated global response to a $CO_2$ increase, and the effect on the thermohaline circulation of a high latitude freshening are quite similar to those of more complex fully coupled atmosphere–ocean general circulation models (Stouffer et al. 2006; Gregory et al. 2005). Note, however, that the coarse-resolution of CLIO and the use of a quasi-geostrophic atmosphere precludes the simulation of phenomena such as El Niño. The Bjerkness coupled air–sea feedback is too weak to amplify sea surface temperature anomalies (Timmermann et al. 2005). Thus, the results presented in this study focus on changes in the mean state of the ocean-climate system due to the imposed albedo changes.

The atmospheric model ECBILT includes a simplified parameterization of radiation that uses prescribed climatological (seasonally varying) total cloud cover taken from the International Satellite Cloud Climatology Project. The use of non-interactive clouds allows modification of the imposed cloud cover (and thus the albedo). Note that a change in the cloud cover does not necessarily imply a change in the total cloud amount. Instead, it amounts to changes in the optical properties of the clouds. In the present climate the high latitudes are dominated by low clouds, which reflect the incoming short wave radiation from the sun. If these stratiform clouds were to be replaced by high clouds the reflecting properties would be different. The albedo effect of high clouds tends to be compensated by the greenhouse effects of the clouds so that the net change in TOA radiation is small. Low clouds, instead, do not trap much long-wave radiation, but reflect a significant portion of the incoming short wave.

The simulations described in this paper include the following:

*Control* — This is a simulation of the basic, unperturbed state.

*EXT0.5* — In this simulation the climatological cloud cover, poleward of 20° latitude in both hemispheres, strictly over the oceans, is reduced by half. There is a linear ramp between 20 and 30°N, S that blends the reduced extratropical cloud cover with the unmodified tropical values. This experiment is run for 1,000 years, by which time the TOA fluxes (and the surface ocean) are essentially in equilibrium, with a heat imbalance of only 0.28 W/m$^2$.

*NP0.5* — This simulation is similar to the previous one but only the cloud cover poleward of 20°N over the Pacific Ocean is reduced. This experiment is run for 500 years.

*SO0.5-35S* — This simulation is similar to *EXTO.5* but only the cloud cover poleward of 35°S is reduced. This experiment is run for 500 years.

*SO0.5-35S_PC20* — Similar to *SO0.5-35S*, but with partial coupling between 20°S and 20°N. In the partial coupling strategy the atmosphere sees climatological SST (from *Control*) between 20°S and 20°N, and the predicted SST everywhere else. The ocean model, on the other hand, is forced with atmospheric fluxes everywhere in the domain (Wu et al. 2004). Thus, in this experiment there is partial ocean–atmosphere coupling within the tropics. This experiment is run for 500 years.

In this study the last 100 years of the runs are used for analysis, unless otherwise noted.

## 3 Climate response to an extratropical decrease in cloud cover

When the cloud albedo over the extratropical oceans is reduced the system responds by decreasing the poleward transport of heat in the ocean and the atmosphere (Fig. 1a). The atmospheric heat transport is reduced in both hemispheres, but particularly in the southern one because the cloud cover reduction is larger there because of a more extensive ocean area. This decrease in atmospheric heat transport is consistent with a weaker SH Hadley cell (as indicated by the vertical velocity at 350 mb) that results form a weaker pole-to-equator temperature gradient (Figs. 1b, 2a). The poleward oceanic heat transport in the northern hemisphere does not change significantly, but it decreases in the southern hemisphere.

The high latitude oceans warm up significantly due to the increased short-wave radiation at the surface (Figs. 2a, 3a). In the absence of any circulation that can transport heat, the ocean will tend to warm up to emit more long-wave radiation and to lose more latent and sensible heat to the atmosphere in order to regain a locally balanced heat budget. This happens to a large extent over the global oceans. However, there are certain regions in which the changes in surface fluxes do not compensate for the increased short wave radiation, namely, the Southern Ocean and the high latitude North Atlantic (Fig. 2b). An inspection of the individual heat flux components shows

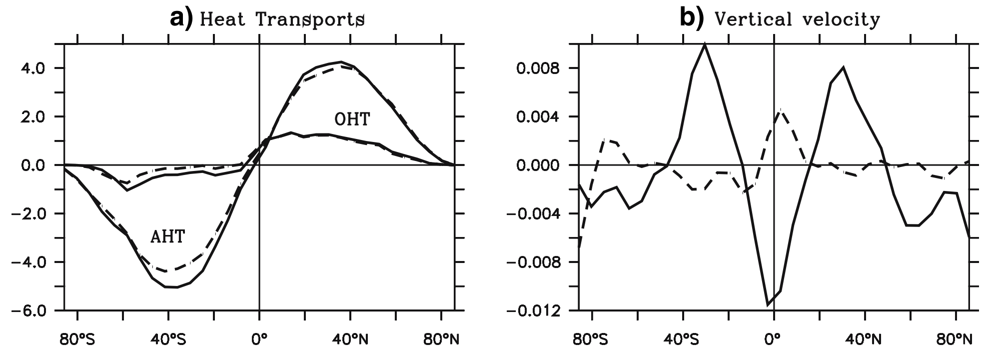


**Fig. 1** **a** Atmospheric and oceanic heat transport in *Control* (*solid*) and *EXT0.5* (*dashed*) experiments. Units are in PW ($10^{15}$ W). **b** Vertical velocity (Pa/s) at 350 mb in *Control* (*solid*) and changes in *EXT0.5* (*dashed*). The vertical velocity shows that the southern hemisphere Hadley cell weakens in *EXT0.5*, consistent with a reduction in the atmospheric heat transport

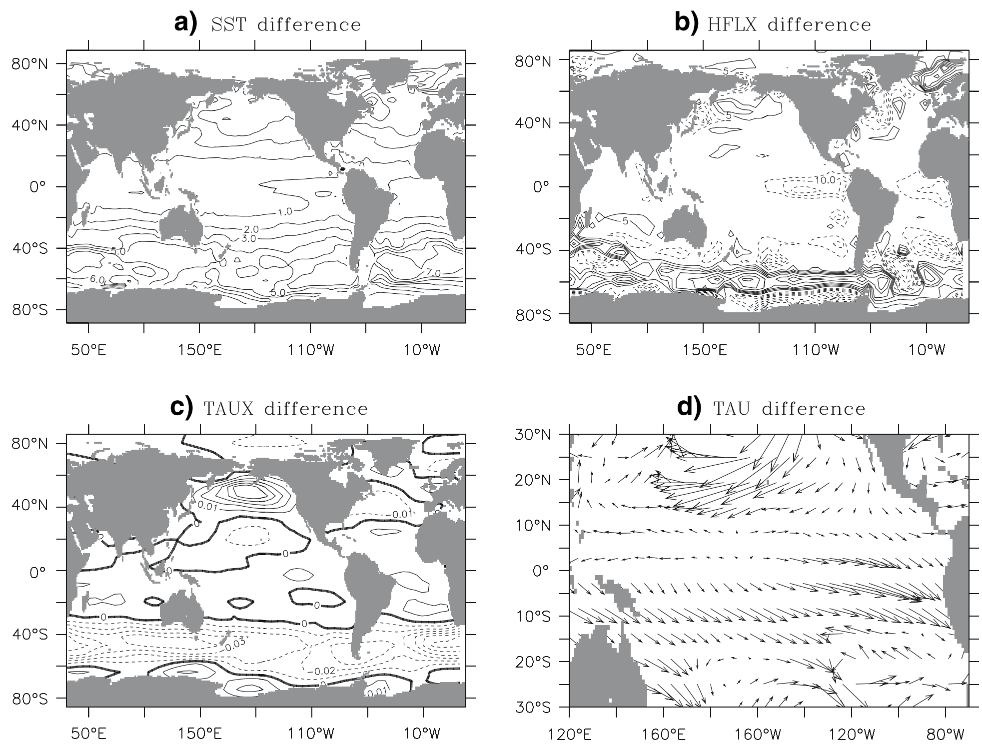


**Fig. 2** Changes in different fields in experiment *EXT0.5* with respect to *Control* conditions: **a** SST (K), **b** net downward surface heat flux (W/m$^2$), **c** zonal wind stress (Pa), and **d** tropical Pacific wind stress (Pa). The contour scale in **b** is [(−20:5:−5) (5:5:20) (−60:10:−20) (20:10:60)]

that these are regions where the ocean is losing less sensible heat to the atmosphere even though the ocean is warmer (Fig. 3). Changes in latent heat flux in these regions are also small. The reason is that in the perturbed experiment the atmosphere warms up more than the ocean in these high latitude regions so that the transfer of sensible heat is reduced. The region next to Antarctica between 160°W and 80°W loses more sensible heat in the perturbed experiment due to the decrease in sea ice (the newly exposed ocean is much warmer than the original sea ice).

These results imply that the ocean loses less heat in the high latitudes when the albedo decreases. Thus, a balanced oceanic heat budget requires a reduced heat gain. There is a tendency for the ocean to gain less heat at about 40°S. Nevertheless, since the regions of heat gain are mainly in the eastern sides of the tropical oceans, the changes in the extratropics imply that the low latitudes must change. This is clearly seen in Fig. 2a, b where the eastern equatorial Pacific and tropical Atlantic become anomalously warm so that they reduce the uptake of heat. Inspection of the different heat flux components reveals that the anomalously warm water of the tropical oceans lose more latent heat to the atmosphere. Figure 4 summarizes the results showing the zonal mean of oceanic surface heat fluxes averaged in the Pacific sector.

The warming of the eastern Pacific reduces the east-west equatorial SST gradient by about 1 K (Fig. 5a). The subsurface equatorial Pacific shows an eastern warming larger than 2 K, while the central and eastern Pacific tend to show smaller changes, signaling a decrease in the zonal slope of the thermocline (Fig. 6).

The reduction of the east-west SST gradient is accompanied by decreased equatorial easterlies, particularly east of the dateline where they decrease a maximum of ∼30%

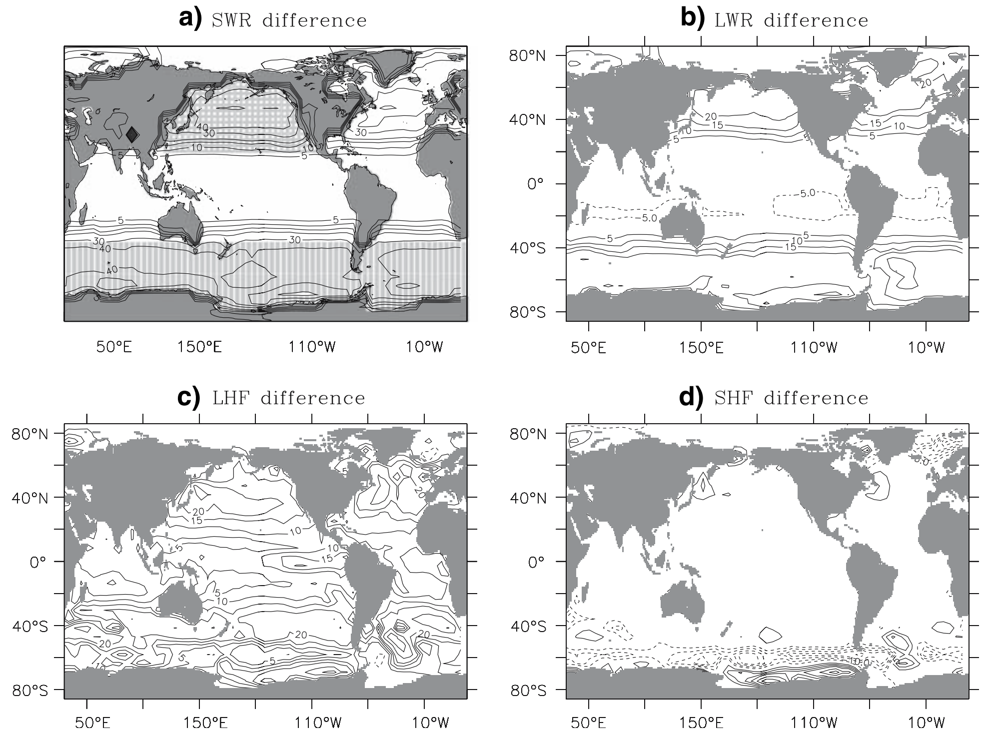


**Fig. 3** Changes in individual surface heat flux components in *EXT0.5* with respect to *Control* (W/m$^2$): **a** net downward short-wave radiation, **b** net outgoing long-wave radiation, **c** latent heat flux, and **d** sensible heat flux. Contour scale as in Fig. 2. The *shadings* denote the regions of cloud reduction in experiments *NP0.5* (*cross hatching*) and *SO0.5-35S* (*vertical hatching*)

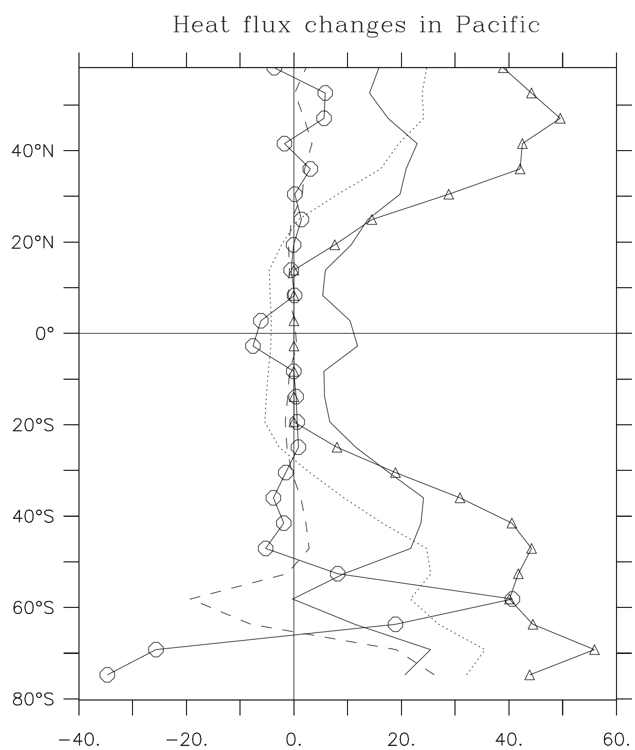


**Fig. 4** Zonal mean changes of oceanic surface heat fluxes in the Pacific sector (150E–90W) in *EXT0.5* with respect to *Control* (W/m$^2$). The plotted fields are the net downward surface flux (*circles*), latent heat flux (*solid*), sensible heat flux (*dashed*), net upward long-wave radiation (dotted), short-wave downward radiation (*triangles*). The net downward surface heat flux is calculated as net = sw − lw − lhf - shf

(Fig. 5b). This decrease extends up to 15°S across the tropical Pacific (Fig. 2d) and is largest next to the South American coast. Over the Southern Ocean there is a large reduction in the surface westerly winds (Fig. 2c). According to the thermal wind relationship westerly winds in the troposphere decrease when the pole-equator temperature gradient decreases. The decreased baroclinicity leads to weaker weather systems, smaller eddy meridional momentum transport, and thus weaker surface winds. There is a small tendency for an equatorward shift of the maximum winds. In the northern Atlantic there is also a weak reduction of the westerly wind stress. In contrast, in the north Pacific the westerlies decrease in the subtropics but increase north of 40°N signaling the presence of anomalous high pressure.

Changes in the surface atmospheric conditions influence the ocean circulation. Figure 7 shows the changes in the meridional overturning circulation over the global oceans. The largest change at the surface is a 10 Sv weakening of the Deacon cell due to reduced zonal wind stress over the Southern ocean that decreases the Ekman divergence (consistent with Rahmstorf and England 1997). The weakening of the southern subtropical cell in Fig. 7 represents the changes in the tropical Pacific due to decreased easterlies that accompany the warmer eastern equatorial Pacific. In the deep ocean there is a substantial decrease of the southward North Atlantic Deep Water outflow even though there are little changes at the surface in the North Atlantic. Thus, the Atlantic meridional overturning circulation tends to weaken and shallow.

**Fig. 5** **a** Equatorial Pacific temperature difference between *EXT0.5* and Control (K), **b** zonal wind stress (Pa) along the equator in EXT0.5 (*solid*) and Control (*dashed*)

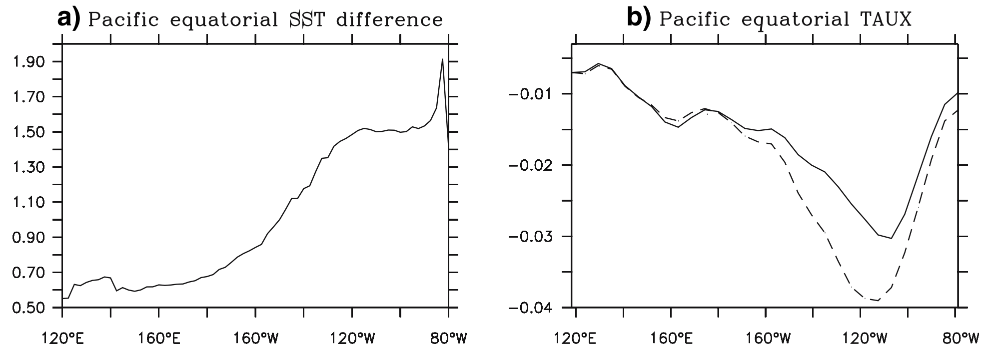


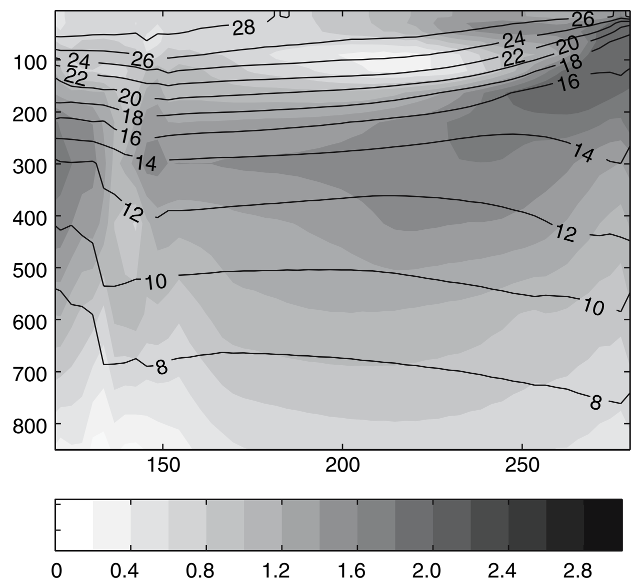


**Fig. 6** Equatorial temperature change (K) in *EXT0.5* with respect to control experiment (*shading*). The lines denote the temperature structure in the unperturbed control case

These results imply that variations in high latitude cloud cover can influence the tropical region, changing the mean state of the equatorial thermocline and the uptake of heat. In the next sections we determine which is the most important region in this connection. We focus on the tropical Pacific and argue that the equatorial changes shown in Fig. 1 are mainly a consequence of reduced cloud cover over the Southern Ocean.

## 4 Changes in North Pacific cloud cover

We isolate the effect of the reduction of cloud albedo over the North Pacific on the tropical region using the output of the experiment *NP0.5* where the cloud cover is modified only north of 20°N in the Pacific Ocean.

As in experiment *EXT0.5*, changes in the net surface heat flux in the North Pacific do not show a clear spatial pattern (Fig. 8). The decrease in cloud cover warms up the ocean, which then emits more long-wave radiation and latent heat that tends to balance the extra incoming solar radiation locally. In contrast with experiment *EXT0.5*, the tropical Pacific shows a small uniform warming resulting from the increased water vapor in the atmosphere, with no change in the zonal SST gradient. As result there are negligible changes in the tropical uptake of heat. These results suggest that the warming of the cold tongue observed in experiment *EXT0.5* does not result from changes in the North Pacific cloud cover. In *NP0.5* the increase in TOA radiative fluxes are balanced only by changes in the atmospheric circulation (and heat transport).

## 5 Changes in Southern Hemisphere cloud cover

In this section we look at the results from experiment *SO0.5-35S*, where the oceanic cloud cover in the Southern Hemisphere south of 35°S is reduced by half its climatological value. At the end of the 500-year run the system is very close to equilibrium: the global mean TOA radiative flux (and surface ocean heat flux) is 0.22 W/m$^2$. Comparison with *EXT0.5* reveals that the changes in SST and heat fluxes in *SO0.5-35S* over the Southern Ocean and Pacific Ocean have the same structure (Fig. 9). There is a surface warming in the Southern Ocean and South Pacific that ranges from 3 to 6 K, and a warming of the eastern equatorial Pacific of about 0.9 K. The western Pacific SST remains largely unchanged in *SO0.5-35S* because the trapping of heat by the water vapor is much smaller than in *EXT0.5*. The decrease of the zonal equatorial SST gradient, however, shows almost the same magnitude in *SO0.5-35S* and *EXT0.5*. Heat flux changes in the Southern Ocean and Pacific cold tongue region are weaker in *SO0.5-35S* because the magnitude of the warming is smaller. Nevertheless, the spatial changes of the individual components of the heat flux are very similar to those in experiment *EXT0.5* south of 35°S and in the Pacific cold tongue region (not shown). Again, the decrease in heat loss in the Southern Ocean is mainly due to a decrease in the sensible heat. This region coincides with that of decreased Ekman upwelling

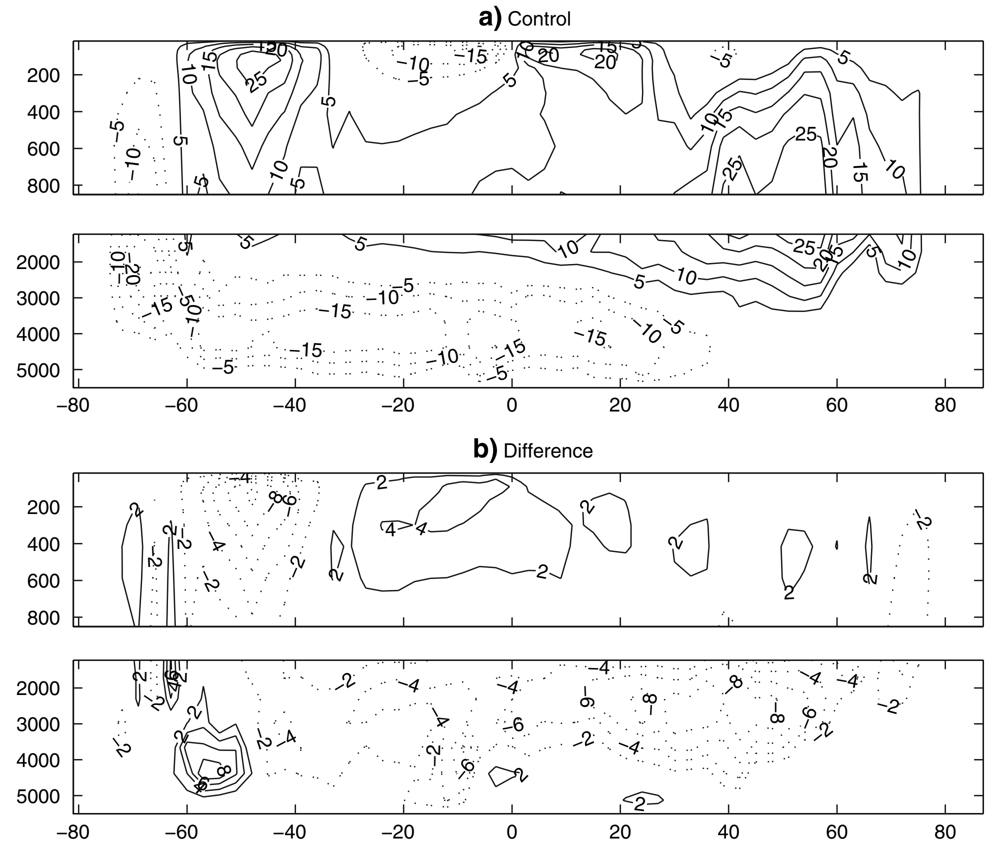

**Fig. 7** **a** Global zonal mean meridional circulation in unperturbed control case and **b** deviations from control in *EXT0.5* experiment. The *upper panel* shows the upper 1,000 m and the *lower panel* the deep ocean. Units are in Sv ($1\ \mathrm{Sv} = 10^6\ \mathrm{m^3/s}$)

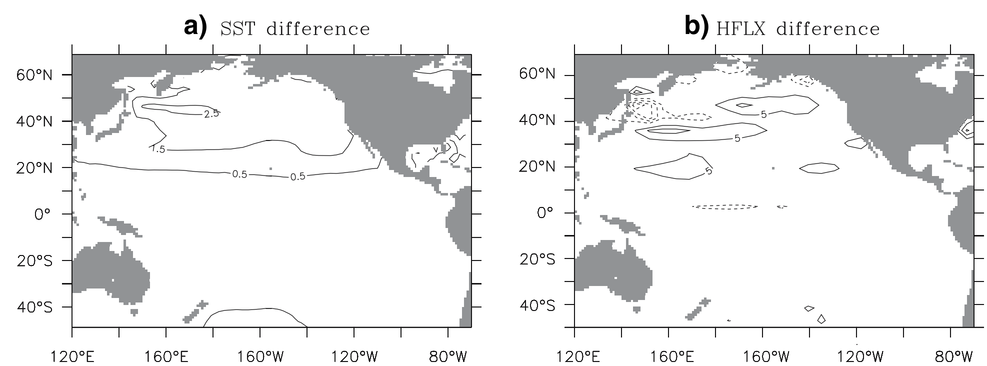

**Fig. 8** Changes in **a** SST (K), and **b** net surface heat flux ($\mathrm{W/m^2}$) in experiment *NP0.5* with respect to control. Note the absence of significant equatorial anomalies

from the deep due to weaker westerlies over the Southern Ocean (Fig. 11b). From these results it is clear that the Pacific tongue region is connected to the southern hemisphere through atmospheric and/or oceanic bridges, and the changes in the heat fluxes in these two remote regions tend to compensate each other so that the ocean maintains a balanced heat budget.

The changes in the vertical structure of the equatorial temperature are shown in Fig. 10a. As expected, it has the same pattern as in *EXT0.5* with smaller magnitude. The zonal mean changes in the Pacific basin show a large warming between 60°S and 30°S that extends from the surface down to 600 m deep north of 50°S and down to 2,000 m south of 50°S (not shown). In the tropics there is a region of cooling at about 10°S between 100 and 200 m deep (Fig. 10b) associated with a southern shift of the ITCZ (Fig. 11a), and that results from increased Ekman upwelling due to changes in the wind stress curl and in the beta-effect term (Figs. 11b, c). The anomalous Sverdrup flow due to changed wind stress tends to decrease the mean depth of the equatorial thermocline adding to the weakening of the equatorial easterlies and results in the cooling anomaly seen in the central Pacific at 100 m in Fig. 10a. Changes in the wind stress curl and in the beta-effect term

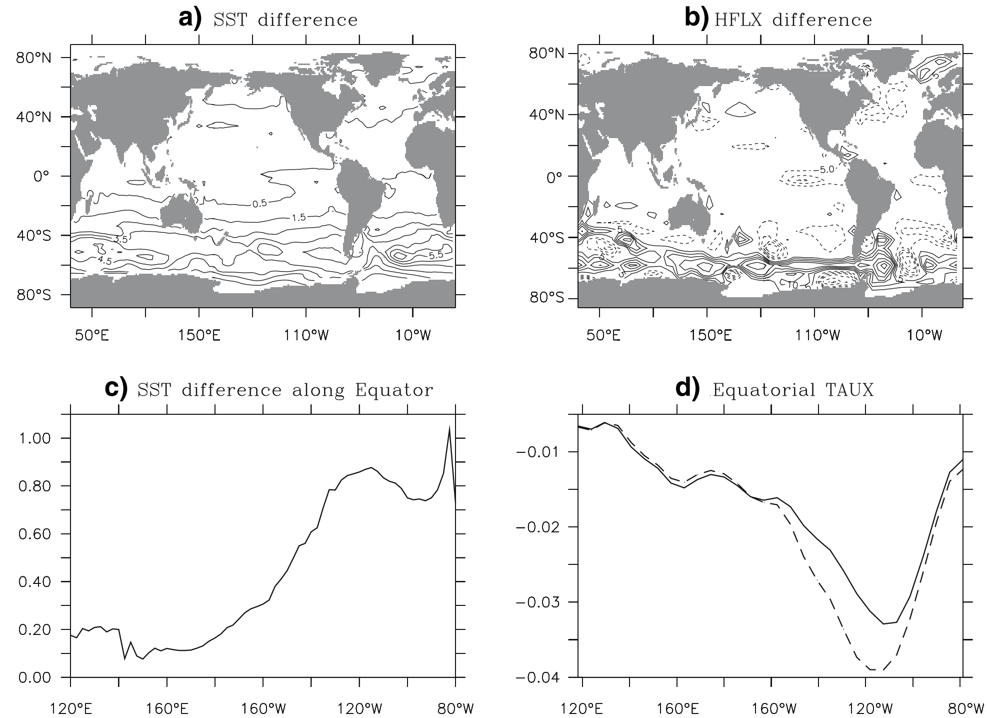


**Fig. 9** Changes in **a** SST (K), and **b** net surface heat flux (W/m$^{2)}$ in experiment *SO0.5-35S* with respect to control. **c** Equatorial Pacific temperature difference (K), **d** Zonal wind stress (Pa) along the equator in SO0.5-35S (*solid*) and control (*dashed*)

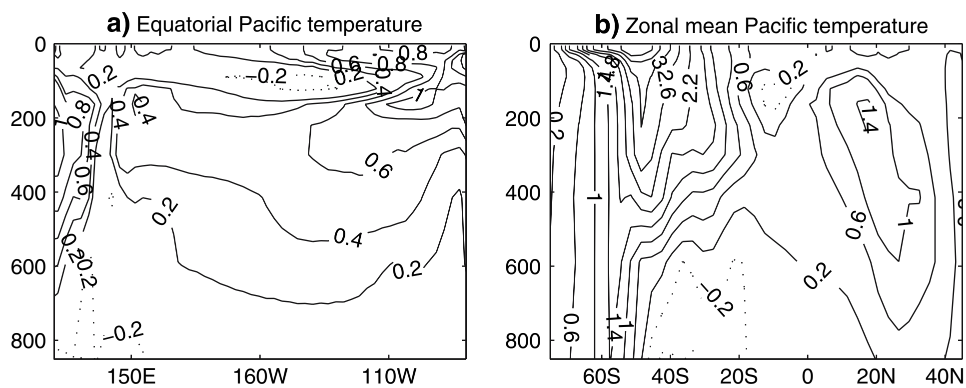


**Fig. 10** **a** Change in equatorial Pacific temperature (K), and **b** in zonal mean Pacific temperature (averaged over [140e–80w]) in experiments *SO0.5-35S* with respect to control

in the northern tropics–subtropics drive anomalous Ekman convergence resulting in the warm subsurface anomaly from 10 to 40°N seen in Fig. 10b.

The changes in the wind stress curl over the southern subtropics weaken the subtropical wind driven cell (Fig. 12). The decrease in the surface zonal and meridional wind stress in the high latitudes of the southern hemisphere is comparable to that in *EXT0.5* (Fig. 13) significantly weakening the Antarctic Circumpolar Current and the upwelling in the Southern Ocean (Figs. 11, 12). The changes in the oceans' meridional volume streamfunction show a corresponding decrease in the intensity of the Deacon cell. In the deep ocean there is a decrease in the southward flow of the North Atlantic meridional overturning circulation (Fig. 12).

## 6 The atmospheric bridge

The previous section showed that the equatorial Pacific is most sensitive to changes in Southern Hemisphere albedo. It is not clear, however, if the signal is transported to the tropics through the atmosphere, the ocean or a combination of both. Also, what role do tropical ocean–atmosphere interactions play?

In this section we asses the role of the atmospheric bridge in connecting the extratropics with the tropical region, using a model consisting in ECBILT coupled to a slab ocean of 80 m deep. We run analogous experiments as with ECBILT-CLIO, that is with 50% decreased cloud cover in the extratropics (*EXT0.5-slab*), only in the North Pacific (*NP0.5-slab*) and only poleward of 35°S (*SO0.5-35S-slab*).

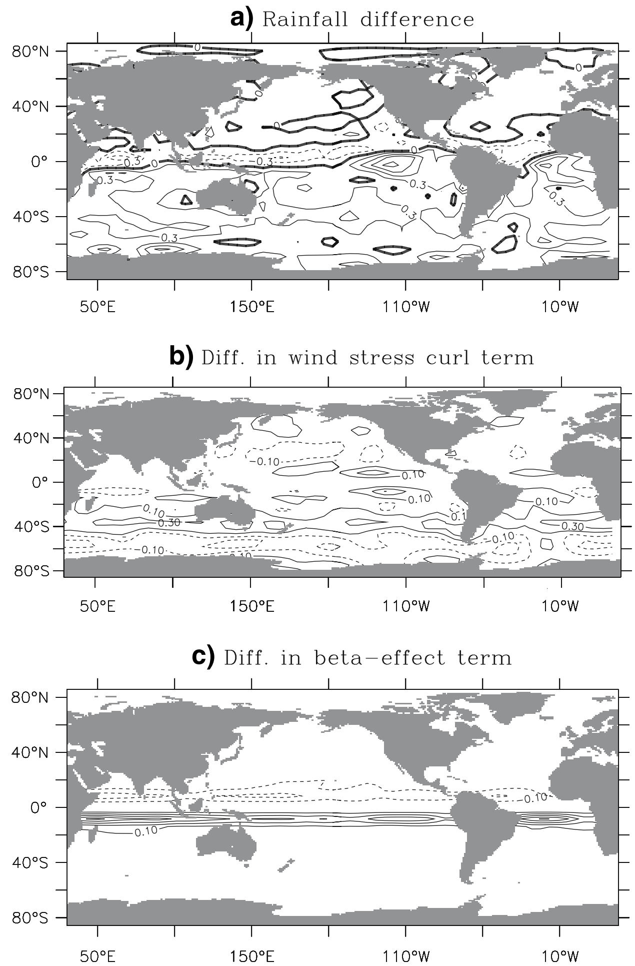


**Fig. 11 a** Change in the precipitation (mm/day) in experiment *SO0.5-35S* with respect to Control. The lower two panels show the changes in Ekman pumping $\rho w_e = \left[\frac{\partial \tau_y/f}{\partial x} - \frac{\partial \tau_x/f}{\partial y}\right]$(kg/m$^2$s) separated in the components, **b** due to the wind stress curl $=\frac{1}{f}\left[\frac{\partial \tau_y}{\partial x} - \frac{\partial \tau_x}{\partial y}\right]$ and **c** due to the beta-effect $\tau_x \frac{\beta}{f}$. In the latitude band 5°S–5°N the Ekman pumping is not defined

These experiments are run for 50 years as the model comes close to an equilibrium already at year 20; the last 20 years are used for analysis. Note that in this model the oceanic heat transport is prescribed using a Q-flux that assures the realistic representation of the climatological SST. The anomalous heat fluxes that results from the change in cloud albedo must then be balanced locally at each grid point.

Comparison of the SST changes in each of the three experiments reveals a similar result as using ECBILT-CLIO: only albedo changes in the southern hemisphere influence the equatorial cold tongue (Fig. 14). Moreover, the experiments demonstrate that the atmospheric bridge plays an important role in this connection, and is done through changes in the Hadley cell. For example, in *EXT0.5-slab* the reduced albedo decreases the pole-to-equator temperature gradient, resulting in a weaker Hadley cell and decreased equatorial easterlies. The decrease in wind speed reduces the latent heat loss warming the surface. At the same time there is reduced long-wave cooling of the ocean's surface due to a warmer and moister atmosphere (Fig. 15). Since the wind speed decreases more in the east than in the west, the initial net heat flux imbalance is largest in the former resulting in larger surface warming. Once the SST is large enough, the latent heat flux changes sign so that the ocean starts loosing more heat, opposing the effect of decreased long-wave cooling. Because of the non-linearity of the Clausius–Clapeyron equation, the latent heat flux increases more slowly in the colder eastern Pacific than in the warmer west (see slopes in Fig. 15). Thus, the eastern Pacific requires a larger warming to regain a locally balanced heat budget (it takes about 15 years in the west and 20 years in the east). As result, in experiment *EXT0.5-slab* the east warms up about 0.4 K more than the west (Fig. 16).

The result that only albedo changes in the southern hemisphere can affect the equatorial cold tongue agrees with YL05, even though the experimental setup is different. On the other hand, using an atmospheric model coupled to a slab, Chiang and Bitz (2005) show that changes in land or sea ice in the northern (as well as in the southern) hemisphere propagate equatorward through a wind-evaporation-SST feedback (Liu and Xie 1994) affecting the equatorial region. Our results suggest this physical mechanism may be operating in our model, but

**Fig. 12** Global zonal mean meridional circulation change in experiment *SO0.5-35S*. The *upper panel* shows the upper 1,000 m and the *lower panel* the deep ocean. The contour interval is 2 Sv

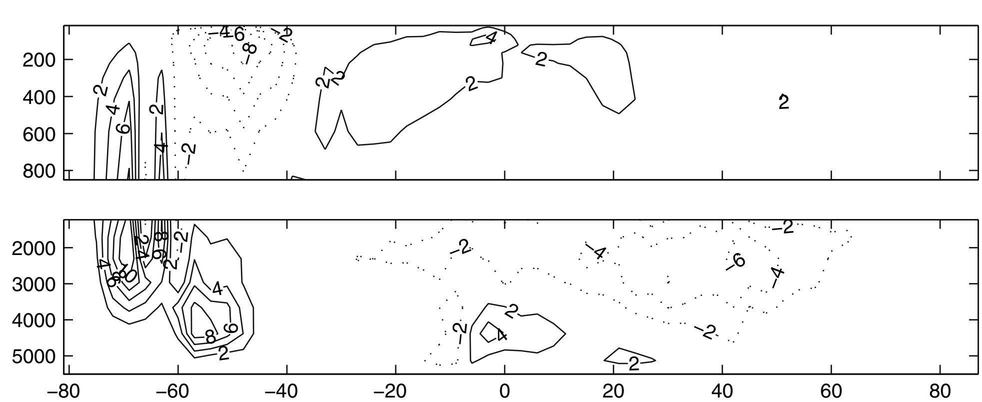

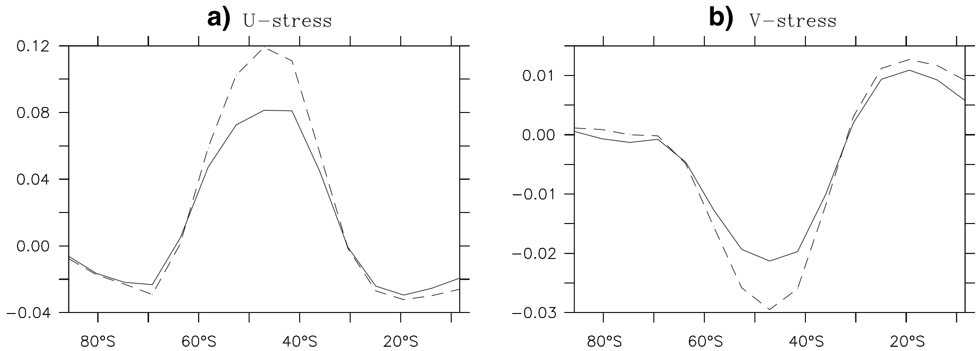


**Fig. 13** Global mean zonal (*left panel*) and meridional (*right panel*) wind stress in *SO0.5-35S* (*solid*) and Control (*dashed*). Units are in Pa

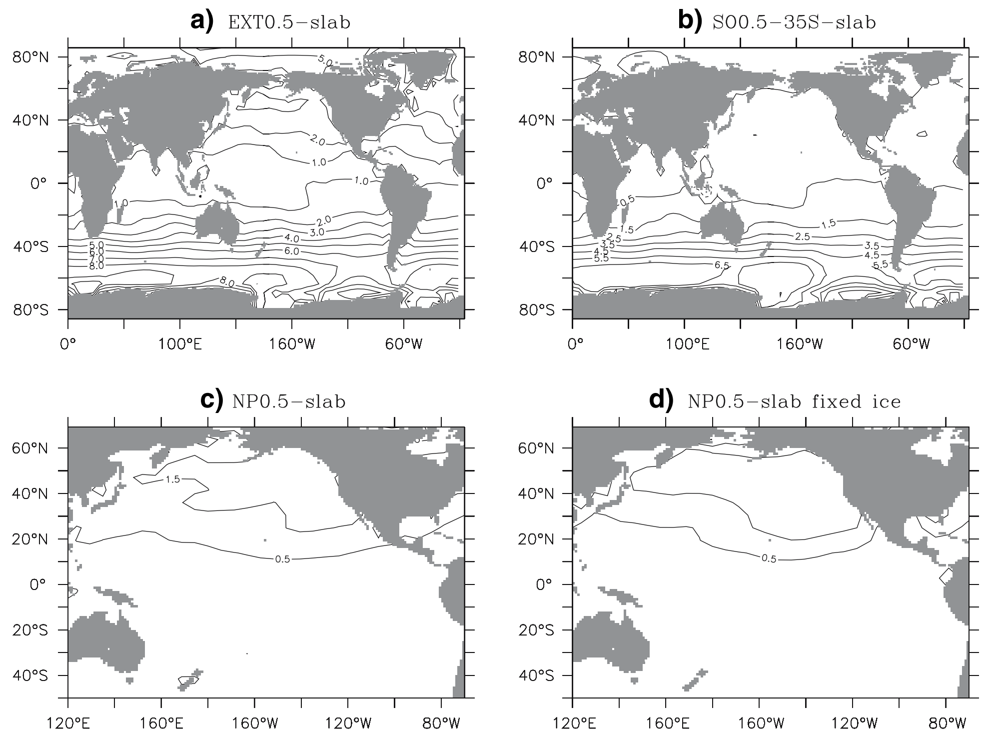


**Fig. 14** Experiments with ECBILT-SLAB. SST changes (K) with respect to Control in **a** *EXT0.5-slab*, **b** *SO0.5-35S-slab*, **c** *NP0.5-slab*, and **d** *NP0.5-slab* with fixed ice. The contour interval is 1 K

only from the southern hemisphere. Chiang and Bitz (2005) used prescribed sea ice, and it may be that sea ice feedbacks are a major reason for this north-south asymmetry in the results. To test this possibility we repeated *NP0.5-slab* with fixed sea ice cover and thickness. Results in this case show that the extratropical warm anomaly caused by decreased albedo becomes more asymmetric in the east-west direction and tends to propagate equatorward in the eastern side of the basin, in closer agreement with results of Chiang and Bitz (2005) (Fig. 14d). However, the anomaly does not reach the equator, and this region shows a uniform warming of 0.15 K as with interactive sea ice (Fig. 16).

## 7 The role of the ocean

The previous section showed that the atmospheric bridge alone accounts for about 40% of the reduction in the east-west equatorial Pacific SST gradient due a thermodynamic effect. The rest of the anomaly in *EXT0.5* must be then related to ocean dynamics, either through the oceanic propagation of the signal from the extratropics or through the coupling with the atmosphere in the tropical region. We focus here on the connection from the southern hemisphere to the equatorial region.

### 7.1 The role of changes in the S.O wind stress

The decreased Southern Hemisphere westerlies in *SO0.5-35S* (Fig. 13) change the oceanic circulation. To isolate the effect of these wind changes in the tropical–extratropical connection we performed an additional experiment in which we run the coupled model with unaltered clouds (albedo), but with the daily varying climatological wind stress taken from experiment *SO0.5-35S* between 30 and

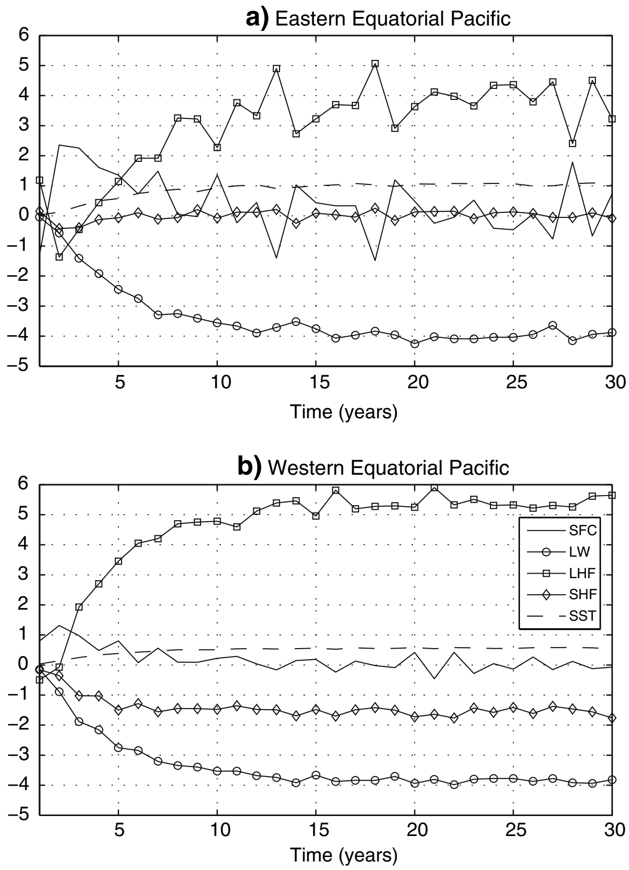


**Fig. 15** Evolution of surface heat flux anomalies in *EXT0.5-slab* in the **a** eastern equatorial Pacific [125W–85W,5S–5N], and **b** western equatorial Pacific [150E–170W,5S:5N]. The *dashed line* shows the evolution of SST. *LW* net surface long-wave radiative flux, *LHF* latent heat flux, *SHF* sensible heat flux, *SFC* net surface heat flux. The short-wave radiation is not plotted because it does not change

70°S (500-year run). Many studies have addressed the influence of the Southern Ocean winds on the ocean general circulation, particularly on the Atlantic Meridional Overturning Circulation (e.g., Toggweiler and Samuels 1993, 1995; Rahmstorf and England 1997). In agreement with these studies we find that the Deacon, Antarctic and bottom cells weaken. Moreover, there is an upper ocean cooling in the upper 1,000 m that signals a shallower pycnocline as predicted by Gnanadesikan (1999). Nevertheless, the tropical shallow cells stay unchanged, and the tropical SST changes are negligible (Fig. 17a). The heat budget is mainly balanced locally in the Southern Hemisphere: As the wind stress is weaker, there is less upwelling of cold water from the deep in the Southern Ocean and the surface ocean cools at about 60°S due to the overlaying colder atmosphere. This also decreases the northward Ekman transport of cold water, which tends to warm up SST at about 40°S. The net heat flux changes accompanying these SST anomalies tend to balance each other (Fig. 17b). The only other region showing significant SST

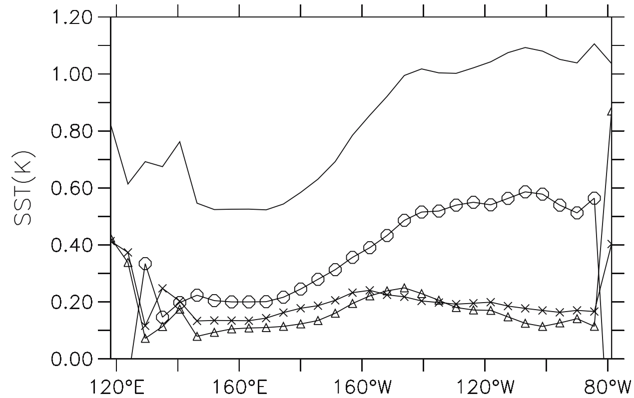


**Fig. 16** SST anomalies in the equatorial Pacific in *EXT0.5-slab* (*solid*), *SO0.5-35S-slab* (*circles*), *NP0.5-slab* (*crosses*), and d) *NP0.5-slab* (*triangles*) with fixed ice cover and thickness. Note that a decrease of North Pacific cloud cover does not change the zonal SST gradient

and heat flux changes is the North Atlantic, which tends to cool when the westerlies in the Southern Hemisphere weaken. This is due to a weakening of the Atlantic meridional overturning circulation and in agreement with the proposed control of north Atlantic deep-water production by the Southern Ocean winds (Toggweiler and Samuels 1995).

## 7.2 Evolution of the equatorial Pacific temperature

According to the previous section the wind changes in the Southern Ocean alone do not influence the equatorial SST. To further understand the role of ocean dynamics we focus on the evolution of the equatorial Pacific temperature anomalies in *SO0.5-35S* (Fig. 18a–c). It can be clearly seen that the surface ocean (above 200 m) adjusts very quickly. The spatial structure after the first 20 years shows the eastern Pacific surface warming and the subsurface central Pacific cooling that already resembles the final anomaly with a smaller amplitude (compare Figs. 18b, 10a). This fast time scale coincides with that of the atmospheric bridge previously found in ECBILT-slab. However, oceanic planetary and coastal waves may also play a role in transporting the extratropical signal (e.g., Kawase 1987; Boccaletti 2005b). Below 200 m the equatorial ocean adjusts much more slowly, with no anomaly present after 20 years into the run. The time series of the surface temperature anomalies indicates that this region has a rapid warming of ~0.4 K with a time scale of 40 years, stays relatively constant up to year 100, and then warms up an additional ~0.1 K. By contrast the equatorial ocean between 250 and 500 m warms up more slowly, with a time scale of about 120 years.

In order to further investigate the ocean adjustment we consider the temperature differences in the initial

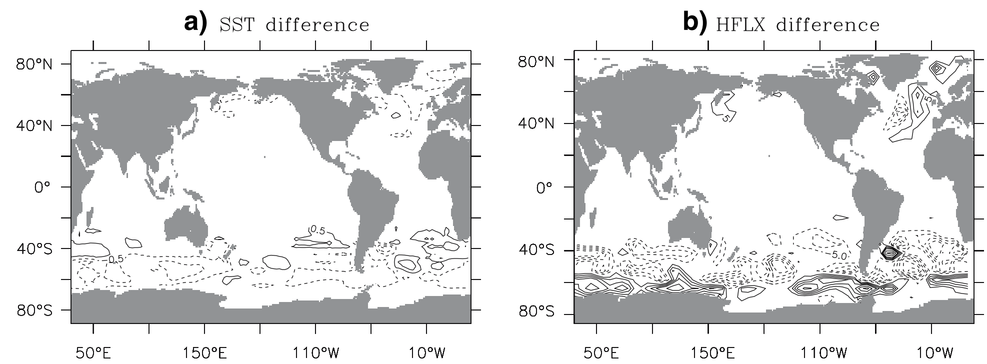


**Fig. 17** Changes with respect to Control in **a** SST (K), and **b** net surface heat flux (W/m$^2$) in experiment with Southern Hemisphere winds taken from *SO0.5-35S*. Contour scale in **b** as in Fig. 2

adjustment phase (1–50 years) and the later phase (61–110) years. Even though we consider two separate phases, the adjustment is consequence of a continuous interplay between the ocean and the atmosphere in the tropical region.

The initial extratropical perturbation that is transported to the tropics will alter the structure of the equatorial thermocline and warm the surface. The adjustment time scale of the equatorial region will be set up by how fast the ocean changes the volume of warm water (or, equivalently, the mean depth of the thermocline), which depends on the changes in wind-driven entrainment and surface heat fluxes (Boccaletti et al. 2005a). Figure 19a, b shows the zonal mean Pacific Ocean temperature changes in the first fast adjustment phase. As mention above, at the surface the eastern Pacific warms up by about 0.5 K, while the central-western Pacific shows a cooling tendency, associated with a decrease in the zonal tilt of the equatorial thermocline. This change in tilt also warms the subsurface of the eastern Pacific because of decreased cold upwelling. Moreover, the Southern Ocean becomes very warm up to a depth of 500 m to the north of 50°S and up to ~2,000 m south of 50°S. This latter warming can also be seen on density coordinates (Fig. 20a), which suggests that both thermocline deepening and propagation of anomalies along isopycnals are responsible for the subsurface warming. In fact, the warming is seen to propagate towards the equatorial region at a depth of about 100–300 m or, equivalently, along isopycnals 1,026–1,027 kg m$^{-3}$. The range of isopycnals that

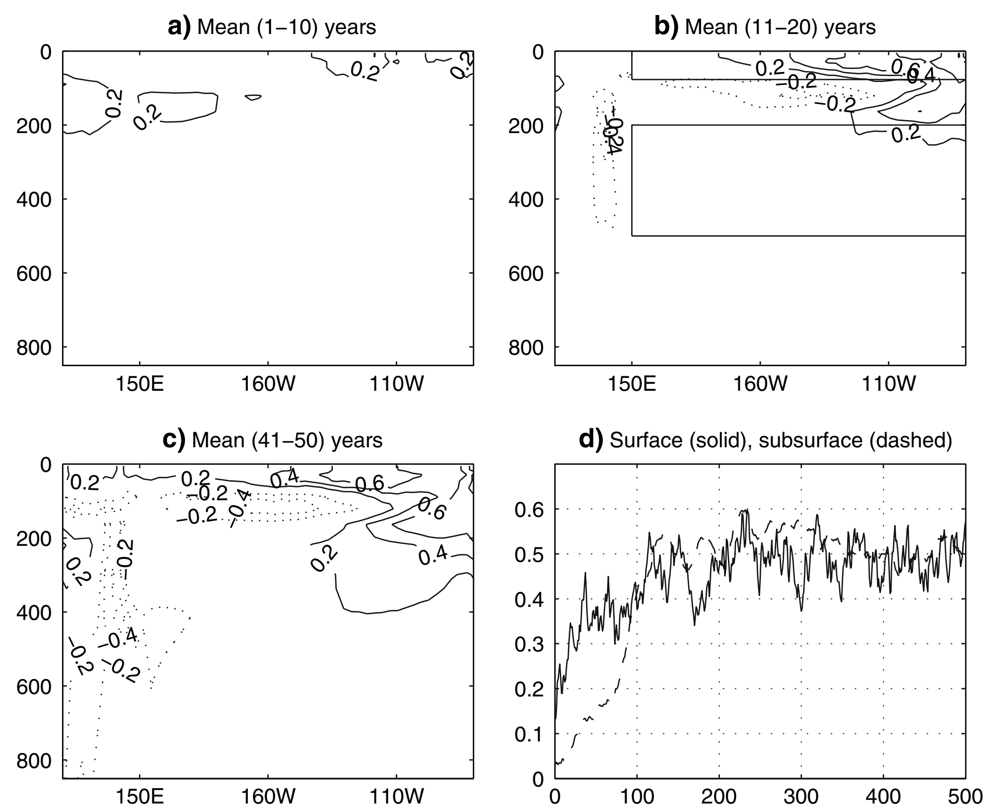


**Fig. 18** Mean equatorial Pacific temperature anomalies (K) in *SO0.5-35S* for years, **a** 1–10, **b** 11–20, and **c** 41–50. **d** Evolution of surface temperature anomalies (*solid*) and subsurface temperature anomalies (*dashed*) in *SO0.5-35S*. The *boxes* in **b** show the regions used for averaging

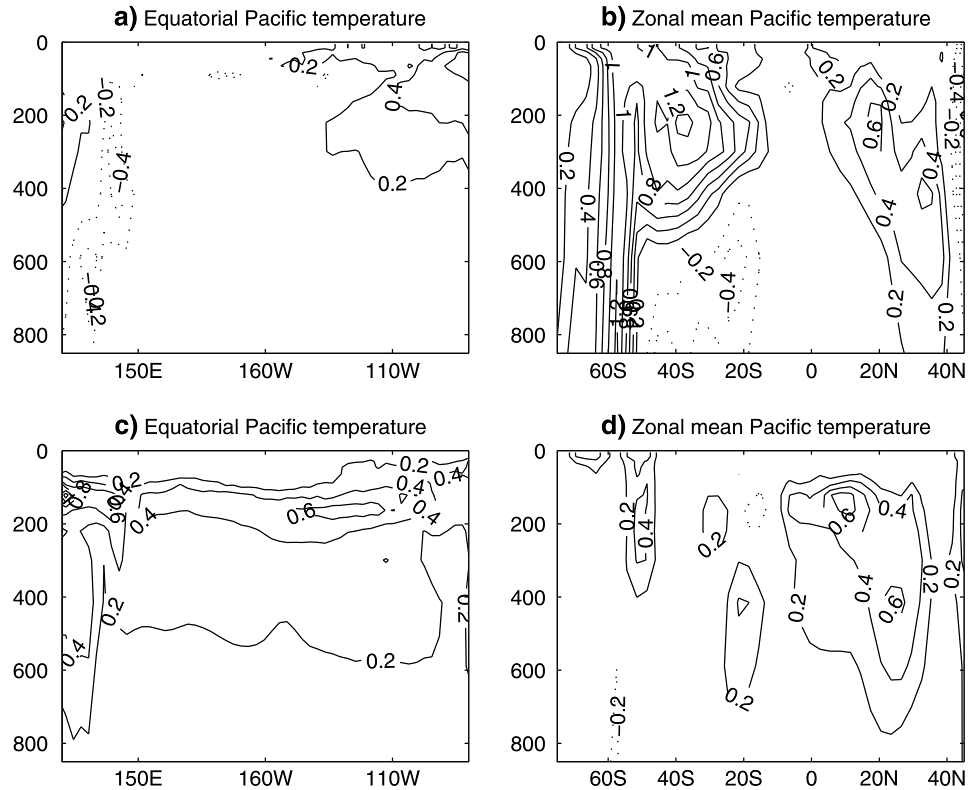


**Fig. 19** Changes in equatorial Pacific temperature (*left column*) and zonal mean Pacific temperature (*right column*) in *SO0.5-35S* with respect to Control. The *upper panels* show the difference between anomalies in years (51–60) and (1–10), and the *lower panels* the difference between anomalies in years (101–110) and (51–60)

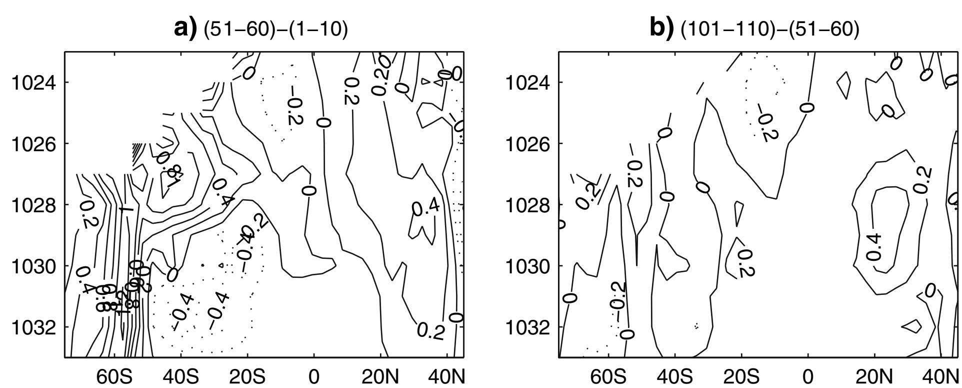


**Fig. 20** Evolution of Pacific zonal mean temperature anomalies (K) along isopycnals in *SO0.5-35S*. **a** Changes between years (51–60) and (1–10), **b** changes between years (101–110) and (51–60)

transmit the signal to the tropics includes the 1026.8 isopycnal that is usually associated with Subantartic Mode Water. This water mass has been identified as the main conduit of nutrients from the Southern Ocean to the upwelling region of eastern Pacific (Sarmiento et al. 2004; Toggweiler et al. 1991), and a possible explanation for the abrupt increase in $\Delta^{14}C$ in the eastern Pacific in 1976/1977 (Rodgers et al. 2004). Nevertheless, the anomalous warming that propagates from the extratropics along the mean thermocline ("oceanic tunnel") has very small amplitude in the equatorial region. Closer to the equator, at about 10°S there is a subsurface cooling (mentioned before), consequence of an increase in Ekman upwelling. This anomalous Ekman upwelling tends to oppose the propagation of the warm anomaly from the south. In the northern tropics Ekman pumping is anomalously large and warms the subsurface by deepening the thermocline and increasing the subduction of warm waters (compare Figs. 19b, 20a).

The latter phase of the adjustment shows a different picture (Fig. 19c, d). After the initial 50 years, the surface ocean doesn't change much more, and thermocline anomalies dominate. A look at the zonally averaged temperature anomalies shows that while changes in the southern hemisphere are small, there is a further warming in the northern tropics that extends into the equatorial region between 100 and 500 m. These temperature anomalies are much smaller along isopycnals than in *z*-coordinates (Fig. 20b) indicating that the subsurface warming is mainly due to a deepening of the thermocline and not due to subduction of warm anomalies from the north. An inspection of the wind stress changes during this period shows an increase in the Ekman pumping between 10 and 30°N due to the continuos adjustment of winds to surface temperature anomalies and their mutual interaction (Fig. 21). At the end of the run (year 500) there is anomalous upwelling south of the Equator, and downwelling in the northern tropics that maintain the changes in the tropical temperature structure (also see Fig. 10).

Thus, the evolution of the equatorial thermocline tends to show first a change in the zonal tilt and overall shallowing of the thermocline (defined as the depth of maximum temperature change with depth). As the winds and ocean interact, there is a deepening of the northern tropical thermocline that extends to the equatorial region and deepens the thermocline there. Overall, however, there is a decrease in the zonal tilt and shallowing of the zonal mean depth of the equatorial thermocline (consistent with Jin 1997).

### 7.3 The role of the tropical ocean atmosphere interactions

We finish the discussion examining the role of the tropical dynamical ocean–atmosphere coupling by comparing the results of *SO0.5-35S* with those of *SO0.5-35S_PC20*. In this latter run, while the ocean sees the full atmospheric winds, the atmosphere does not see the SST changes within 20°S–20°N. Thus, air–sea coupling in the tropics is disabled. The experiment is run for 500 years.

Changes in the sea surface temperature with disabled air–sea coupling in the tropical region have a similar spatial structure to those with full interaction (Fig. 22). The southern hemisphere warms up, and the equatorial Pacific cold tongue is reduced with similar magnitude as in *SO0.5-35S*. Nevertheless, the effect of air sea coupling can be clearly seen in the equatorial wind stress changes. Without the coupling, the wind stress weakens slightly, uniformly along the equator, a consequence of the wind adjustment to the changes in pole-to-equator temperature gradient (Fig. 22d). When the coupling is allowed, the warmer eastern Pacific further decrease the easterlies in the eastern side of the basin. As a consequence, the surface equatorial warming becomes more concentrated in the eastern Pacific, while the western side shows only a small warming (Fig. 22b).

The subsurface changes are also different (Fig. 23), a consequence of the different evolution of the wind stress. With the coupling disabled the Ekman suction to the south of the equator is weaker and develops later in the run, allowing the intrusion of warm water from the south (not shown). In the northern tropics wind stress curl anomalies are very small, particularly north of 10°N where the anomalous downwelling present in *SO0.5-35S* is now all but absent (Fig. 22c), resulting in a smaller warming between 200 and 800 m. In this experiment, the equatorial subsurface has not yet reached an equilibrium and has a small cooling tendency, which may be due in part to the anomalous Ekman suction at 10°N (not shown).

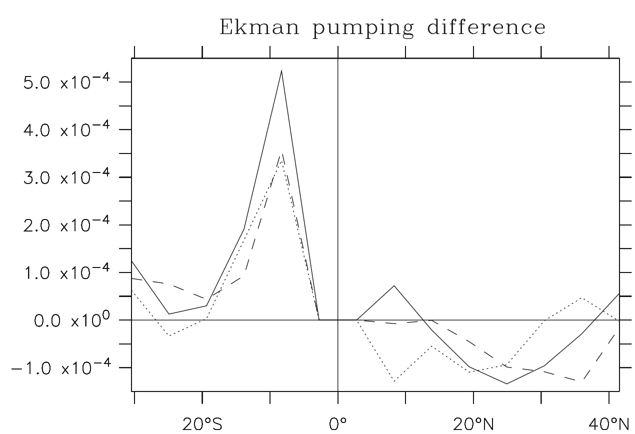


**Fig. 21** Zonal mean Pacific Ekman pumping anomaly (kg/m$^2$s) in *SO0.5-35S* in years (51–60) (*dashed*), (101–110) (*dotted*), and (401–500) (*solid*). Means are taken over (140°E–90°W)

## 8 Summary

This study explores the response of the climate system to an extratropical reduction in cloud albedo using an intermediate complexity coupled model in which cloud cover can be prescribed. We found that the response includes a warming of the eastern equatorial cold tongues, that is linked to changes in the Southern ocean conditions, in agreement with previous works (YL05). When the cloud albedo is decreased south of 35°S the Southern Ocean warms up and the eastern Pacific cold tongue decreases due to a local deepening of the thermocline. The connection between low and high latitudes can be thought as consequence of the constraint of a balanced oceanic heat budget. The increase in short wave due to the reduction in cloud cover decreases the heat loss in the high latitudes mainly by decreasing the loss of sensible heat flux from the ocean. In order to recover a balanced heat budget, the ocean deepens its equatorial thermocline, warming the eastern Pacific and losing more latent heat flux to the atmosphere. Nevertheless, it is important to keep in mind that the main constraint of an equilibrated climate system is balancing the radiative fluxes at the top of the atmosphere. The adjustment of the coupled atmosphere–ocean to changes in cloud albedo could have consisted of changes in atmospheric circulation only, as is the case in the experiments (with ECBILT-slab)

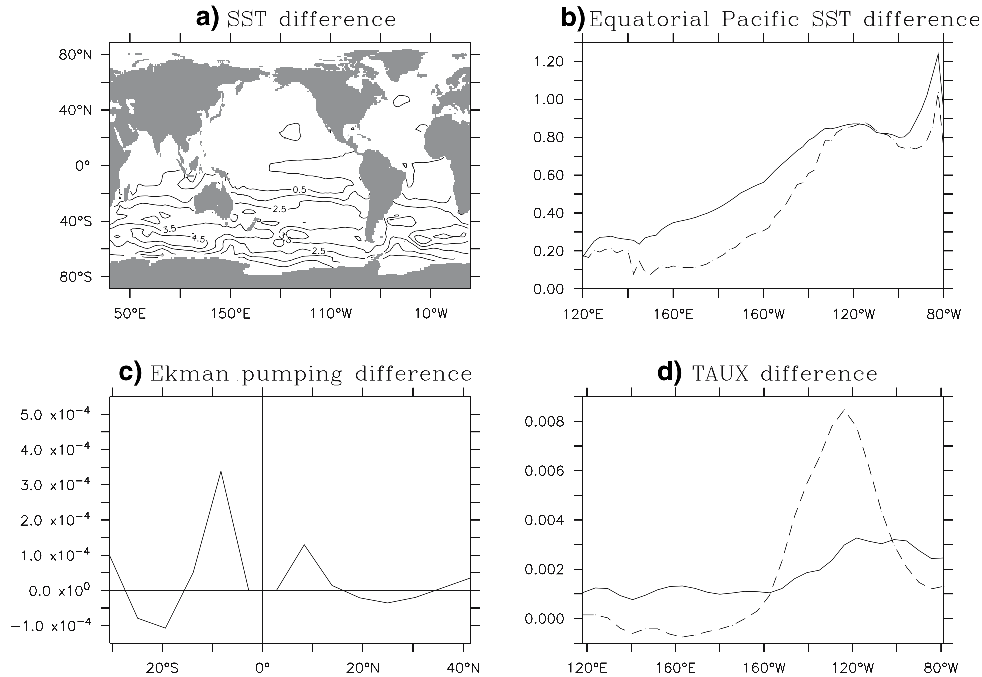


**Fig. 22** Deviations from Control in experiment *SO0.5-35S-PC20*. **a** SST (K), **b** Equatorial Pacific SST (K, *solid*), **c** zonal mean Pacific wind stress curl (140°E–90°W), and **d** equatorial Pacific wind stress (Pa, *solid*). In **b** and **d** the dashed lines denote the changes in *SO0.5-35S*

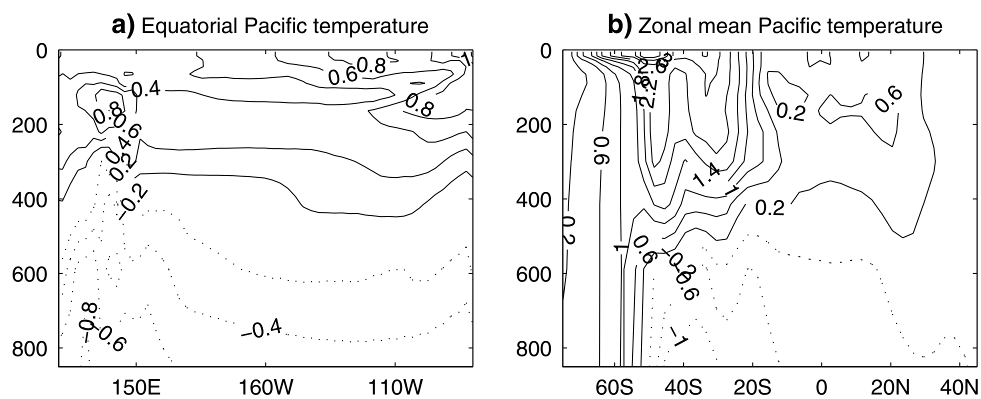


**Fig. 23** **a** Change in equatorial Pacific temperature (K), and **b** in zonal mean Pacific temperature in experiments *SO0.5-35S-PC20* with respect to control

in which the ocean is motionless. In the real world, however, this does not happen because changes in the atmospheric circulation modify the ocean circulation through wind stress changes. Thus, the general response to a perturbation in the cloud albedo depends on ocean–atmosphere interactions.

The connection from the extra-tropics to the tropics can be through oceanic and atmospheric processes. In the experiments described here the atmospheric bridge plays an important role, while the oceanic tunnel from the extratropics, on the other hand, tends to play a small role. Nevertheless, oceanic waves may also propagate the extratropical signal to the tropics (Boccaletti 2005b). Once the signal arrives, the tropical ocean starts to adjust interacting with the winds. The time-scale on which the equatorial cold tongue warms up and the zonal tilt and mean depth of the equatorial thermocline decreases is on the order of $\sim$40 years and is controlled by changes in upwelling and surface heat fluxes. The adjustment continues as the tropical sea surface temperatures increase because of changes in the off-equatorial winds and in the Ekman pumping. An increase in anomalous Ekman pumping in the northern tropics deepens the thermocline and further warms the subsurface equatorial region. As a result, the equatorial sea surface temperatures in the Pacific adjusts in about 120 years.

The decreased cloud cover in the Southern Hemisphere weakens significantly the westerlies over the Southern Ocean, weakening the Antarctic Circumpolar Current, the upwelling and its associated Deacon cell. In agreement with previous studies, there is also a weakening of the Antartic bottom cell, and of the southward flow of the Atlantic meridional overturning circulation at about 2,000 m.

A new possibility for abrupt climate change connects the Southern Ocean and the tropical Pacific on interdecadal time scales: were the cloud albedo to decrease, the tropical Pacific would respond by deepening the eastern equatorial thermocline and decreasing the east-west SST gradient. Further simulations with other climate models are needed to test the sensitivity of this connection on the model used.

The study of YL05 addressed the influence of the extratropics on the tropical climate by prescribing sea surface temperatures poleward of 30° in a coupled model. They found that the prescription of a 2 K anomaly in the extratropics, that could represent the response due to a doubling of atmospheric $CO_2$, induces a tropical warming of about 1 K. In our experiments, we found that decreasing the extratropical cloud cover by half induces a 1.5 K warming in the eastern Pacific. It is important to note, however, that there is a significant difference between our results and those of YL05. In our case, the tropical response to an extratropical warming resulted in a decrease of the east-west equatorial SST gradient; in YL05 the warming is almost uniform and there is a slight increase of this gradient. The decrease in the east-west sea surface temperature gradient due to a thermodynamic effect is already present when ECBILT is coupled to a slab ocean, and this mechanism likely works in the model of YL05. Thus, either the different experimental setup and/or representation of the ocean dynamics induces a different equatorial response. YL05 suggest that the increased west-east gradient results from the existence of the "ocean dynamical thermostat" in their model. As mentioned before, the Bjerkness feedback is too weak in ECBILT-CLIO, which could hinder the existence of the thermostat mechanism. On the other hand, a doubling of the atmospheric concentration of $CO_2$ induces in ECBILT-CLIO a response similar to that of the several IPCC models, namely a slight reduction of the equatorial sea surface temperature gradient along the equator east-west gradient, whereas the model of YL05, and some IPCC models tend to increase that gradient (Liu et al. 2005). At present there is no agreement about the response of the tropical Pacific to an increase in the concentration of greenhouse gases (Collins et al. 2005; Liu et al. 2005).

The results of this study have interesting applications to past climates, especially the Pliocene when, as mentioned in the introduction, extratropical regions were about 3 to 6 K warmer than today, and cold surface waters were absent from the equatorial Pacific and coastal upwelling regions. (The global configuration of continents, and the atmospheric concentration of carbon dioxide, were essentially the same as today.) Presently, low clouds dominate in the extratropical latitudes where they reflect a large portion of the incoming short-wave radiation. Thus, our findings suggest that reduced extratropical cloud cover, and hence a reduced albedo, contributed to the warm conditions of the middle Pliocene.

The results presented here may also be relevant to the Earth's response to variations in obliquity. The obliquity of the Earth's orbit changes the distribution of incoming solar radiation, increasing and decreasing the extratropical short-wave radiative flux with a period of about 41.000 years. Thus, obliquity could in principle produce the simulated response described in this study, and there are in fact some indications of a co-evolution of the Pacific cold tongue on these time scales (Fedorov et al. 2006).

Finally, and coming back to the present day, were the greenhouse forcing to modify the extratropical clouds and albedo, our results suggest that it would be accompanied by a change in the equatorial Pacific thermocline. This may afterwards induce further climate changes by changing the properties of El Niño (Fedorov and Philander 2000; Zhang et al. 2005).

**Acknowledgments** The authors would like to thank K. Rodgers for helpful discussions, and the comments of two anonymous reviewers that greatly improved the manuscript. This study was supported by grants from NASA (NA86GP0338), NASA/JPL (NM0710772), NOAA (NA17RJ2612 NA003OAR4310065) and by CSIR and NRF (South Africa).

## References

Barreiro M, Fedorov A, Pacanowski R, Philander SG (2007) Abrupt climate changes: how freshening of the northern Atlantic affects the thermohaline and wind-driven oceanic circulations. Annu Rev Earth Planet Sci (in press)

Boccaletti G, Pacanowski RC, Philander SG, Fedorov A (2004) The thermal structure of the upper ocean. J Phys Oceanogr 34:888–902

Boccaletti G, Pacanowski RC, Philander SG (2005a) A diabatic mechanism for decadal variability in the tropics. Dyn Atmos Oceans 39:3–19

Boccaletti G (2005b) Timescales and dynamics of the formation of a thermocline. Dyn Atmos Oceans 39:21–40

Chiang JCH., Bitz C (2005) Influence of high latitude ice cover on the marine intertropical convergence zone. Clim Dyn. doi: 10.1007/s00382-005-0040-5

Clement A, Cane MA, Zebiak S (1996) An oceanic dynamic thermostat. J Clim 9:2190–2196

Collins M, CMIP Modelling Group (2005) El Niño- or La Niña-like climate change?, Clim Dyn 24:89–104

Fedorov AV, Philander SG (2000) Is El Nino changing? Science 288:1997–2002

Fedorov AV, Dekens PS, McCarthy M, Ravelo AC, deMenocal PB, Barreiro M, Pacanowski RC, Philander SG (2006) The Pliocene Paradox (Mechanisms for a Permanent El Niño). Science 312:1485–1489

Gnanadesikan A (1999) A simple theory for the structure of the oceanic pycnocline. Science 283:2077–2079

Goose H, Fichefet T (1999) Importance of ice-ocean interaction for the global ocean circulation: a model study. J Geophys Res 104(C10):23337–23355

Gregory JM et al (2005) A model intercomparison to changes in the Atlantic thermohaline circulation in response to increasing atmospheric $CO_2$ concentration. Geophys Res Lett 32:L12703. doi:10.1029/2005GL023209

Gu D-G, Philander SGH (1997) Interdecadal climate fluctuations that depend on exchanges between the tropics and extratropics. Science 275:805–807

Jin F-F (1997) An equatorial ocean recharge paradigm for ENSO. Part I: conceptual Model. J Atmos Sci 54:811–829

Kawase M (1987) Establishment of deep circulation driven by deep-water production. J Phys Oceanogr 17:2294–2317

Kirk-Davidoff DB, Schrag DP, Anderson GJ (2002) On the feedback of stratospheric clouds on polar climate. Geophys Res Lett 29(11):1556. doi:10.1029/2002GL014659

Knutti R, Flackiger J, Stocker TF, Timmermann A (2004) Strong hemispheric coupling of glacial climate through freshwater discharge and ocean circulation. Nature 430:851–856

Liu Z, Xie S-P (1994), Equatorward propagation of coupled air–sea disturbances with application to the annual cycle of the eastern tropical Pacific. J Atmos Sci 51:3807–3822

Liu Z, Yang H (2003) Extratropical control of tropical climate, the atmospheric bridge and oceanic tunnel. Geophys Res Lett 30(5). doi:10.1029/2002GL016492

Liu Z, Vavrus S, He F, Wen N, Zhong Y (2005) Rethinking tropical ocean response to global warming: the enhanced equatorial warming. J Clim 18:4684–4700

Manabe S, Stouffer RJ (1995) Simulation of abrupt climate change induced by freshwater input to the North Atlantic ocean. Nature 378:165–167

Meskhidze N, Nenes A (2006) Phytoplankton and cloudiness in the Southern Ocean. Science 314:1419–1423

Opsteegh JD, Haarsma RJ, Selten FM, Kattenberg A (1998) ECBILT: a dynamic alternative to mixed boundary conditions in ocean models. Tellus A 50:348–367

Rahmstorf S (1995) Bifurcation of the Atlantic thermohaline circulation in response to changes in the hydrological cycle. Nature 378:145–149

Rahmstorf S, England MH (1997) Influence of Southern Hemisphere winds on North Atlantic Deep Water flow. J Phys Oceanogr 27:2040–2054

Rodgers KB, Aumont O, Madec G, Menkes C, Blanke B, Monfray P, Orr JC, Shrag DP (2004) Radiocarbon as a thermocline proxy for the eastern equatorial Pacific. Geophys Res Lett 31.doi: 10.1029/2004GL019764

Sarmiento JL, Gruber N, Brzezinski MA, Dunne JP (2004) High latitude controls of thermocline nutrients and low latitude biological productivity. Nature 427:56–60

Sloan LC, Pollard D (1998) Polar stratospheric clouds: a high latitude warming mechanism in an ancient greenhouse world. Geophys Res Lett 25(18):3517–3520

Stouffer RJ et al (2006) Investigating the causes of the response of the thermohaline circulation to past and future climate changes. J Clim 19:698–722

Sun D-Z, Zhang T, Shin S-I (2004) The effect of subtropical cooling on the amplitude of ENSO: a numerical study. J Clim 17:3786–3798

Timmermann A, Goosse H (2004a) Is the wind stress forcing essential for the meridional overturning circulation? Geophys Res Lett 31:L04303. doi:10.1029/2003GL018777

Timmermann A, Justino Barbosa F, Jin F-F, Goosse H (2004b) Surface temperature control in the North Pacific during the last glacial maximum. Clim Dyn 23:353–370. doi:10.1007/s00382-004-0434-9

Timmermann A, An S-I, Krebs U, Goose H (2005) ENSO suppresion due to weakening of the North Atlantic thermohaline circulation. J Clim 18:3122–3139

Toggweiler JR, Samuels B (1993) Is the magnitude of the deep outflow from the Atlantic ocean actually governed by the southern hemisphere winds? In: The global carbon cycle. Springer, Heidelberg, pp 303–331

Toggweiler JR, Samuels B (1995) Effect of the Drake passage on the global thermohaline circulation. Deep Sea Res I 42(4):477–500

Toggweiler JR, Dixon K, Broecker WS (1991) The Peru upwelling and the ventilation of the South Pacific thermocline. J Geophys Res 96:20467–20497

Vellinga M, Woods RA (2002) Global climatic impacts of a collapse of the Atlantic thermohaline circulation. Clim Change 54:251–267

Walker JCG (1995) There is more to climate than carbon dioxide. Rev Geophys 33:205–212. doi:10.1029/95RG00346

Wu L, Zhang Q, Liu Z (2004) Toward understanding tropical Atlantic variability using coupled modeling surgery. In: Earth's Climate: the ocean–atmosphere interaction, Geophys. Monog. 147, American Geophysical Union, pp 157–170

Yang H, Liu Z (2005) Tropical–extratropical climate interactions as revealed in idealized coupled climate model experiments. Clim Dyn. doi:10.1007/s00382-005-0021-8

Zhang Q, Yang H, Zhong Y, Wang D (2005) An idealized study of the impact of extratropical climate change on El Nino-Southern Oscillation. Clim Dyn 25:869–880. doi:10.1007/s00382-005-0062-z